2012

A Near-Neighbor Statistical Survey of the Environments of Galaxies with Water Masers

Thomas Redpath
James Madison University, redpatth@dukes.jmu.edu

Anca Constantin
James Madison University, constaax@jmu.edu

Nathan DiDomenico
James Madison University, natedid@gmail.com

James Corcoran
James Madison University, corcorjj@dukes.jmu.edu

Follow this and additional works at: https://scholarworks.wm.edu/caaurj

A Near-Neighbor Statistical Survey of the Environments of Galaxies with Water Masers

Cover Page Note

1.   Introduction: Megamasers, Galactic Nuclear Activity and Environments

Astrophysical masers are natural microwave amplifiers by stimulated emission. Extragalactic water megamasers are the hugely luminous (brightness temperatures to 10^{16} K) analogs of masers detected in warm ($300 - 1000$ K), dense ($10^7 - 10^{11}$ cm^{-3}) gas, in envelopes of late-type stars and star-formation regions throughout the Milky Way. Water mega-maser emission is revealed predominantly in galaxies hosting Active Galactic Nuclei (AGN), i.e., galaxies whose nuclei are believed to be powered by matter swirling around a supermassive black hole ($M_{\rm bh} > 10^7 M_{\rm sun}$). Less than 40% of them appear in a disk-like configuration (e.g. Kondratko et al. 2006), where the maser spots are associated with central, typically parsec-sized molecular accretion disks, and their spectra show redshifted and blueshifted features in addition to the systemic velocity components.

Water megamasers in disk configurations around central supermassive black holes can provide extremely accurate geometric distance determinations without the need for indirect assumptions about the cosmology/geometry of the universe, and they allow for very accurate calculations of masses of supermassive black holes. A prime example of such measurements used Very Long Baseline Array (VLBA) observations of the maser disk emission in the nearby Seyfert 2 galaxy NGC 4258 (Herrnstein et al. 1999; Miyoshi et al. 2005), which yielded an extremely accurate distance measurement for NGC 4258, $d = 7.2 \pm 0.5$ Mpc, and probably the first highly compelling evidence for the existence of a thin Keplerian disk (e.g., Greenhill et al. 1995), and thus for the existence of a supermassive ($\sim 10^7 M_\odot$) BH (Miyoshi et al. 2005).

Unfortunately, out of more than 3000 objects surveyed for maser emission to date, only 146 galaxies were found to exhibit this type of activity, and only a handful of them are found to be mega-masers in the requisite disk-like configuration (e.g., the Megamaser Cosmology Project, MCP; Reid et al. 2009; Braatz et al. 2010; Kuo et al. 2011). In order to aid the continuing search effort for a statistical sample of mega-maser disks we need to better understand the process by which masers come to exist in galaxy centers, along with the properties of galaxies hosting masers.

We focus here on the environmental properties of galaxies that exhibit

maser emission. Local environment has important consequences on galaxy morphology (Dressler 1980; Georgakakis et al. 2008; Schawinski 2009), star-formation intensities and rates (e.g., Bower et al. 2006), and AGN properties (e.g., Kauffmann et al. 2004; Constantin & Vogeley 2006; Constantin et al. 2008; Silverman et al. 2009). Thus, if maser emission is related to AGN and star-formation activities, the masing phenomenon should also be influenced by the environment. By comparing both the small and the large scale environmental properties between samples of galaxies with and without masers, we investigate here the degree to which various environmental properties affect the maser activity.

Our investigation involves a simple near-neighbor statistical analysis in which the environmental characteristics are measured and quantified via distances to the first, third, fifth and tenth optical neighbors as well as by counts of the number of neighbors within defined search volumes of 0.5, 1, 5 and 10 Mpc radii, for both maser galaxies and those where no maser emission was detected (hereafter referred to as the control sample). We also compile and compare the absolute brightness and the $u - r$ color distributions for neighbors of the maser and control samples. The statistics required for such an investigation are only now available as we make use of the newly public data archive provided by MCP and the Sloan Digital Sky Survey (SDSS; DR7).

Throughout this work we assume a ΛCDM (cold dark matter) cosmology with $\Omega_m = 0.3, \Omega_\Lambda = 0.7, H_0 = 72h$ km s^{-1} Mpc^{-1}.

2. Data

This section describes the maser and the control galaxy samples along with the techniques we used to identify and characterize their neighbors and the methods used in quantifying the environmental properties.

The MCP makes publicly available the list of all galaxies that have been surveyed for maser activity as well as a list of galaxies in which maser activity has been detected. The latest update of the MCP catalogs make available lists of 146 galaxies with maser detections, and a total of 3587 entries for galaxies surveyed for maser activity.

2.1.   Sample Definition

To assemble the lists of maser and control galaxies whose environments can be investigated, we matched objects from the MCP maser and control lists to the SDSS photometric and spectroscopic catalogs, for a search radius of 36″ around the position of each MCP object. When multiple matches were found, we chose the SDSS object with the smallest angular separation from the given maser or control galaxy position, after careful visual examination of all of the matches. The final result of this search consists of 50 maser galaxies and 1227 control galaxies with spectroscopic redshifts (spec-z) and $r < 17.7$; we show as a separate distribution the subsample of maser galaxies for which $L_{\mathrm{H_2O}} > 10 L_\odot$ (i.e., the mega-masers; 38 objects). The main reason for a rigorous visual examination of the cross-matching results is to make sure we extract measurements associated with the galaxy center surveyed for maser activity and not one of the "children" or subregions of nearby large galaxies which are often catalogued by the SDSS automated data reduction pipeline as individual separate galaxies. Table 1 summarizes the number statistics involved in the samples used in this analysis.

Sample	# of Objects
Maser	50
Megamaser	38
Control	1227

Table 1: Number of objects in each sample

As with all comparisons between maser and control galaxies presented in this study, we chose to also show separately the properties of the sub-sample of mega-masers, as these particular systems most often exhibit the disk configuration of interest for distance and black hole mass determination. The properties of the maser sample as a whole are of interest since: 1) masers can vary significantly in intensity (e.g. Felli et al. 2007; Lo 2005) making it very likely that some maser galaxies are hosting mega-masers caught in their low state, which do not appear luminous enough to be classified as mega-masers at the time they are detected, 2) the water maser luminosities, which determine the classification as a mega-maser, are calculated under the assumption of isotropic emission, which is the best accepted model; however, these luminosities are
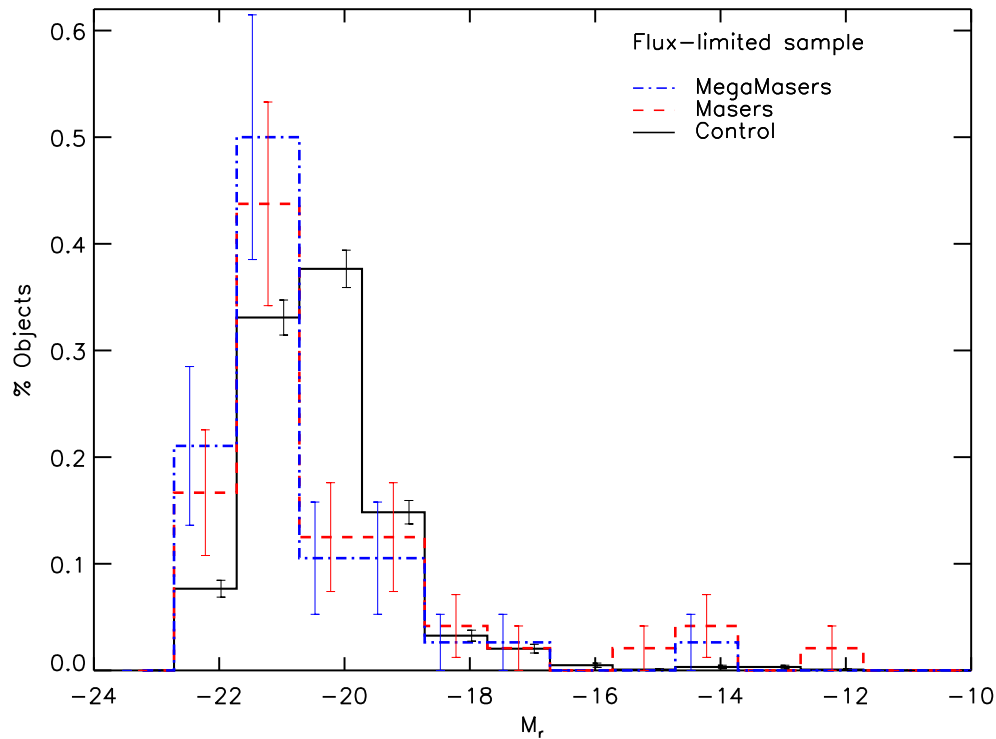
Fig. 1.— Comparison of M_r distributions for maser, mega-maser and control galaxies, shown as red (dashed), blue (dot-dashed), and continuous (black) lines respectively. Error bars show the Poisson standard error in each bin for the mega-maser, maser and control samples, from left to right respectively; they have been shifted for better illustration purposes. The mega-maser galaxies tend to be slightly brighter than the control galaxies which suggests that they are also more massive and probably reside in denser environments.

not indicative of "true" maser luminosity since the masers are beamed into some unknown angle in most cases, and 3) there are better number statistics for the whole maser sample.

Figure 1 shows the distributions of the absolute r-band magnitude M_r for the maser, mega-maser, and control galaxies with SDSS counterparts. This comparison suggests that galaxies hosting mega-masers (median $M_r = -21.1$) tend to be brighter than those where no maser emission was detected (median $M_r = -20.5$), which is consistent with the recent results of Zhu et al. (2011).

However, while the masers span the whole range of brightness, only the kilo-masers ($L_{\mathrm{H_2O}} < 10 L_\odot$) are found in lower luminosity systems.
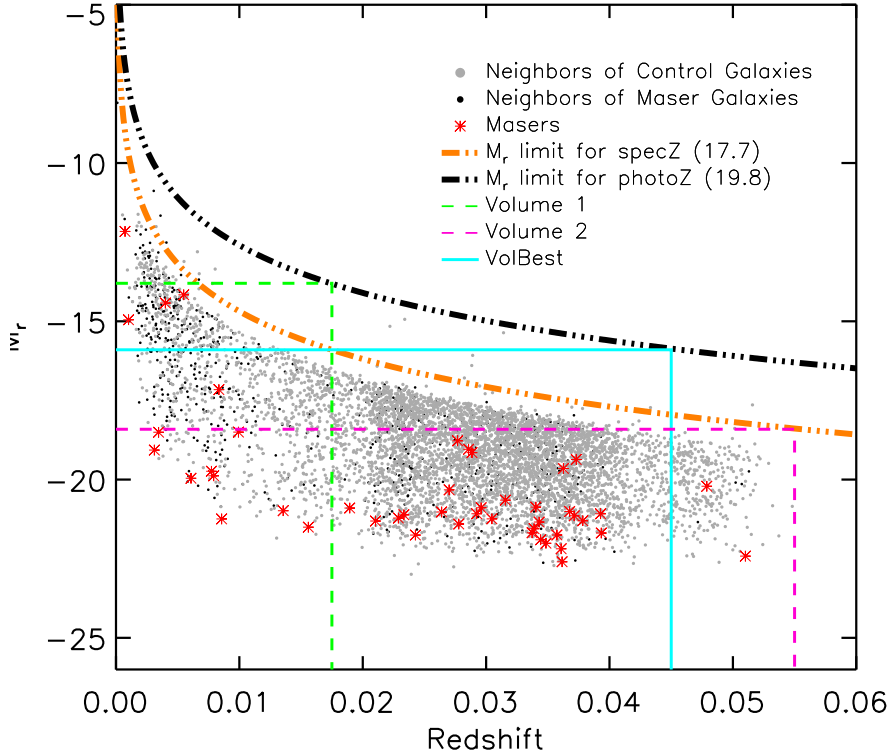

Fig. 2.— Absolute magnitude M_r versus redshift z plot for a randomly chosen subsample of 10% of all the neighbors of maser and control galaxies. For illustration purposes, we also show the maser galaxies (red asterisks). The apparent magnitude limit for the spec-z sample as a function of redshift is indicated by the orange double-dot-dashed line and the corresponding limit for the photo-z sample is indicated by the black double-dot-dashed line; the dashed lines indicate the limits of the volumes considered in this analysis (Volume 1, Volume 2, and VolBest) for three different ranges in redshift.

Initially, we searched for neighbors to each maser and control object in a magnitude-limited ($r < 17.7$) volume, i.e., we searched for all of the neighbors with spectroscopic redshifts (spec-z). For this sample definition, galaxies in the nearby universe will appear to have more neighbors than their more distant

Volume ID	M_r	z
VolBest	-15.9	0.045
Volume 1	-13.8	0.018
Volume 2	-18.4	0.055

Table 2: M_r and z constraints for three volume-limited samples

counterparts since faint galaxies are harder to detect at higher redshifts. In order to adjust for these radial-selection effects, we also consider the neighbor search and characterization in three volume-limited samples drawn from the original flux-limited lists, as described in Table 2 and Figure 2. While the number statistics decrease significantly when working with the volume limited samples, we found no discernible difference from the results of the comparative analysis conducted with magnitude limited samples. We therefore chose to present here the results of the flux-limited analysis.

2.2. Neighbor Searches

The neighbor search process is summarized in Figure 3. To compile the list of neighbors to the maser and control galaxies, we first identified all SDSS objects classified via spectral analysis as galaxies (type = 3 and SpecClass = 2) with $u < 22, g < 22, r < 22, i < 21, z < 20.5$, which define the nominal flux limit for SDSS photometry. The search is initially limited to a projected circular area of radius $R = 10$ Mpc around each galaxy, i.e.

$$\arccos(\sin \delta_n \sin \delta_g + \cos \delta_n \cos \delta_g \cos(\alpha_n - \alpha_g)) < \arctan R/d_g \qquad (1)$$

where α and δ represent the equatorial coordinates (ra and dec) of the target maser or control galaxy (g) and its neighbors (n), R is the 10 Mpc search radius, and d_g is the distance to the target galaxy at (α_g, δ_g). To further reduce the total number of potential neighbors and thus minimize the total size of archival data that is searched for neighbors, we also constrain the redshift difference between a galaxy and its potential neighbors to $\Delta z = 2.4 \times 10^{-3}$, which corresponds to a 10 Mpc physical distance at $z = 0$ with $H_0 = 72h$ km s^{-1} Mpc^{-1}. This choice limits the neighbor search process to a preliminary cylindrical volume centered on each target.

It is often the case that the search volumes for two galaxies overlap, and thus the neighbors within the overlapping volume appear multiple times in the total neighbor list. In the cases where a single galaxy (maser or otherwise) was found to be a neighbor of multiple target galaxies (maser or control) we counted it once for each target to which it is a neighbor, not once overall. Note that for the purpose of our analysis, this choice is necessary to completely characterize the environments of *each* target galaxy. We use the term "entry" to refer to elements of the neighbor lists even though some elements identify the same object as a neighbor of more than one galaxy in our maser and/or control samples.

In order to define the final spherical search volumes for our near neighbor statistical analysis, we calculated the physical distances between each neighbor and its target (maser or control galaxy). We have used the coordinates on the unit sphere from the Hierarchical Triangular Mesh (HTM) code[1], and calculated luminosity distance (d_L) values to derive the x,y,z coordinate values for all galaxies, and thus the physical distances between the target galaxies and all of their neighbors. The d_L values are calculated using the Friedmann-Robertson-Walker model as described in Carroll et al. (1992), p. 511, with the currently accepted ΛCDM cosmology. These distances were then used to define the final total number of neighbors within a radius of 10 Mpc. The list of spec-z neighbors to masers contains 11,438 entries; the list of neighbors of the control galaxies contains 196,634 entries. Future work will incorporate the photo-z neighbors (9,508 neighbors to masers; 182,690 to control) into our analysis, but here we restrict our discussion to the spec-z neighbors.

The next subsections describe the methods we used to identify and discard the false neighbor identifications among the spec-z neighbor entries. The large number of objects in both the maser and control neighbor lists makes visually inspecting each object a laborious task. We describe here the techniques by which we attempted to identify and remove the contaminating artifacts and children.

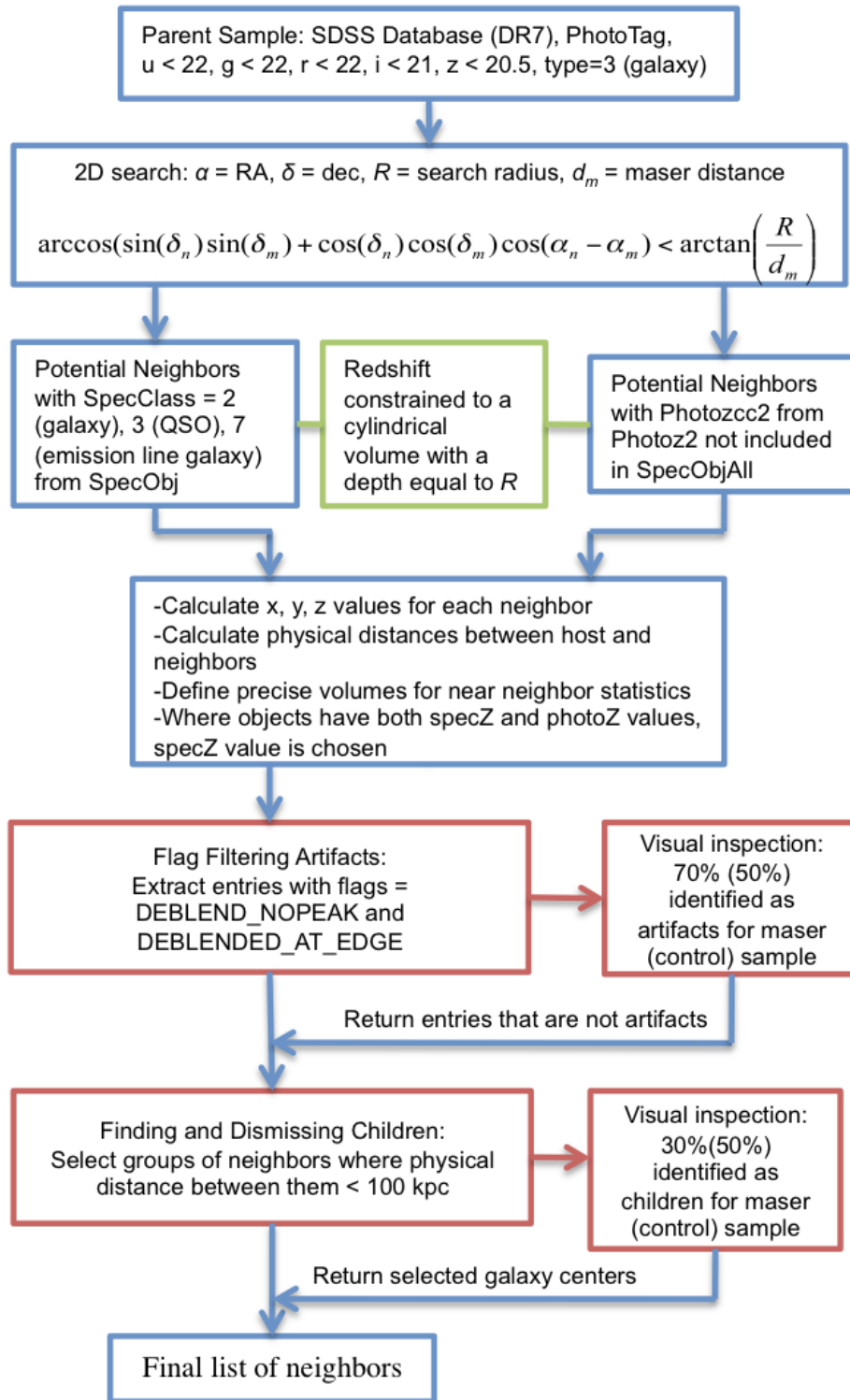[1]see http://www.sdss.jhu.edu/htm/

Fig. 3.— A flow chart depicting the neighbor search process. Percentages in the visual inspection boxes are of the lists extracted by each filtering process.

2.2.1. Removing Artifacts

In order to remove cosmic ray strikes, non-central regions of nearby galaxies and the glow from nearby stars, we identified among the list of potential neighbors those objects flagged by the SDSS analysis with both the DEBLEND_NOPEAK and DEBLENDED_AT_EDGE labels[2]. These two flags were chosen based on the results of flag identification of a wide variety of artifacts identified visually in large randomly sampled subsets of neighbors. These flags are set by survey operations on a frame-by-frame basis and describe the quality of the data[3]. The DEBLEND_NOPEAK flag is set when the SDSS deblending process (which attempts to resolve overlapping objects) detects no peak in at least one of the photometric passbands. The DEBLENDED_AT_EDGE flag is set for objects that appear close to the edge of the frame and have been deblended. A new visual inspection of the flagged objects recovered a few systems that were legitimate neighbor galaxies, and these were returned to the neighbor list. For the spec-z neighbor lists, this process removed 279 (2.4%) entries from the list of neighbors to masers and 553 (0.3%) entries from the neighbors of control galaxies.

2.2.2. Addressing the 'Children' Problem

For systems in the nearby universe, the SDSS automated analysis pipeline identified some regions (e.g., star-forming regions, planetary nebulae, supernova remnants) of some galaxies as individual galaxies (see Figure 4). Inclusion of these "children" would bias the neighbor counts and skew the near-neighbor statistical analysis. To minimize this problem, we identified and removed as many children as possible from the initial lists of neighbor entries.

To identify the children, we compiled sub-lists of neighbors within 100 kpc of each other (i.e., a Milky Way-sized galaxy), and visually inspected them to select the objects that are galaxy centers; we returned the latter objects to

---

[2]Some examples of artifacts included in our initial neighbor list are identified by the following SDSS ObjIDs: 587733399708041281, 587735666377949295, 588017704003895299, and 587725818016563208, see http://cas.sdss.org/dr7/en/tools/explore/obj.asp

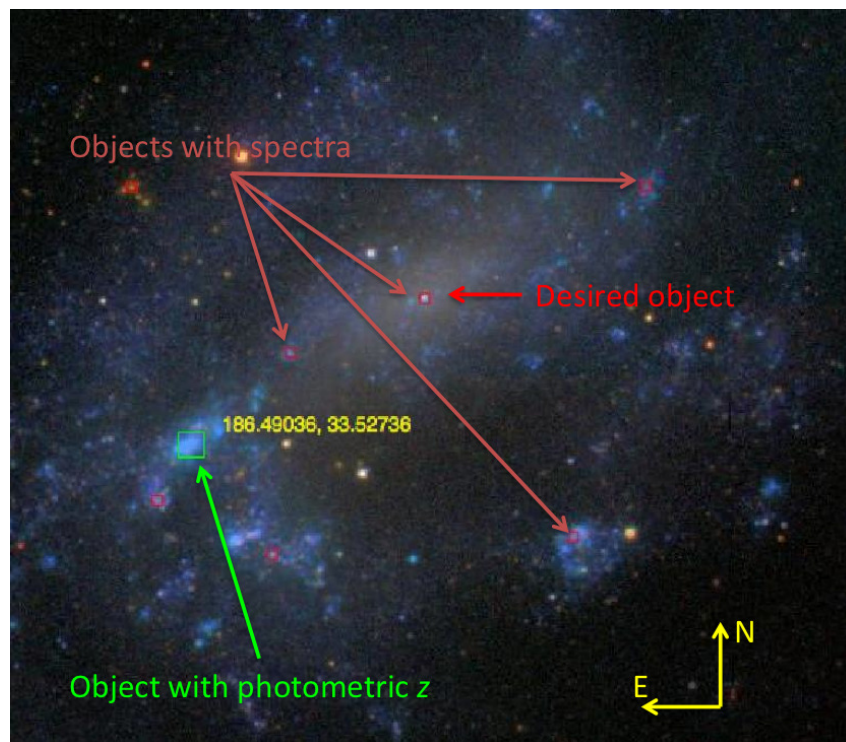[3]see http://cas.sdss.org/astrodr7/en/help/browser/browser.asp

Fig. 4.— An example of a galaxy (SDSS J122548.86+333248.7) for which the SDSS automated analysis pipeline has marked several sub-galactic regions (a.k.a. children) as separate galaxies. The small red boxes denote objects with spectra and the green square denotes an object for which only photometric redshift data is available.

the neighbor lists and discarded the rest. This process removed 144 children from the maser spec-z neighbor list, and 228 children from the control spec-z neighbor list. This translates into a possible children pollution of 1.2% of the maser spec-z neighbor list and $< 1 \times 10^{-3}\%$ of the control neighbor list.

3. Near-neighbor Analysis

In order to quantify the types of environments in which maser galaxies are found and compare them to those of the control, we calculate distances to the nth nearest neighbor, corresponding average densities, and neighbor color and brightness distributions. It should be noted that each of the nearest neighbor

distances (d_{nn}) are intended as separate metrics for characterizing galaxy environments. It therefore makes little sense to compare, for example, the maser d_{1nn} distribution to the other maser d_{nn} distributions, in their absolute values. Similarly for the parameters explored in fixed-volumes (e.g. neighbor counts, M_r, color), the most important comparisons are between the sample properties in a given volume.

3.1.   Distances to n^{th} nearest neighbor

Figure 5 shows distances to the first, third, fifth and tenth nearest spec$-z$ neighbors (d_{nn}) for the flux-limited survey. The d_{nn} metrics provide a means of comparing the small and large scale environmental densities between collections of galaxies, which in this case are the three separate groups of mega-masers, masers, and control galaxies. Smaller d_{nn} values would suggest a
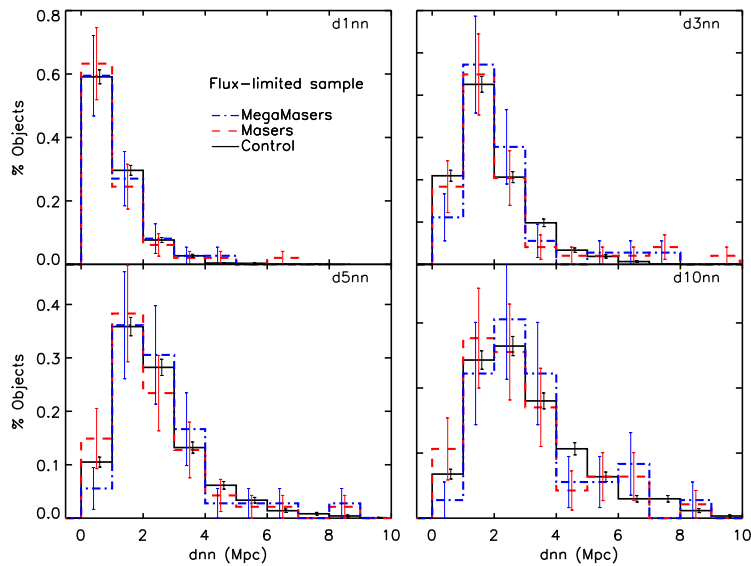

Fig. 5.— Histograms of distances to the $1^{st}, 3^{rd}, 5^{th}$ and 10th nearest spec-z neighbors (d_{1nn}, d_{3nn}, d_{5nn} and d_{10nn} respectively) for the flux-limited samples of mega-maser, maser and control objects. Color/linestyle schemes and error bars are the same as described in the caption of Figure 1.

higher likelihood to exist in denser environments and thus be associated with galaxy interactions. Our comparison shows that there is no apparent difference between the mega-maser/maser and control d_{1nn}, d_{3nn}, d_{5nn} and d_{10nn} distributions; average and median values are consistent with the same value given the associated standard deviations of the means. Thus, to a first approximation, the environments of galaxies with and without maser activity in their center are practically identical.

3.2.   Densities for fixed volumes

Another way of quantifying the environmental properties of these galaxies based on near-neighbor statistics is via computation and comparison of the volume of a sphere with a fixed radius. We employ two different ways to calculate the number densities and investigate the properties of the associated neighbors:

1. The radius is set equal to the distance to the nth nearest neighbor, and thus we obtain the average number densities corresponding to the volumes defined by the nearest $1^{st}, 3^{rd}, 5^{th}$ and 10th spec$-z$ neighbor:

$$\langle \rho \rangle = \frac{N}{\frac{4}{3}\pi R^3} \qquad (2)$$

   where R is the distance to the nth nearest neighbor and N is the number of neighbors with distances less than R (i.e. $N = 2$ corresponds to d_{1nn}).

2. The radius of the spherical volume is fixed to a certain value (0.5, 1, 5 and 10 Mpc) around each maser or control galaxy regardless of how far away the nth nearest neighbors are. With these different volume sizes we are investigating environmental properties at both small and large scales, without constraining the analysis to a specific n^{th} near neighbor.

These average densities are listed in Table 3. These measurements suggest that, especially at small scales (characterized by d_{1nn}), the maser and mega-maser galaxies inhabit less dense regions than those galaxies that do not exhibit maser activity in their centers, although further analysis with larger number

statistics is needed to fully assess the validity of this trend. The densities of the larger scale environments, i.e., calculated based on distances to the 5th and the 10th nearest neighbor, become indistinguishable. Nevertheless, the environments of the mega-maser galaxies stand out as the most rarefied, i.e., show the smallest $\langle \rho \rangle$ values. It is thus possible that the close interactions (e.g., mergers, tidal interactions) play a non-significant role in triggering of maser emission, while the more global, larger scale galactic habitat has neutral effects. In the next subsection we provide a more in depth investigation of the distribution and the properties of the close companions of mega-masers, masers and control galaxies.

Sample	$R = d_{1\mathrm{nn}}$	$R = d_{3\mathrm{nn}}$	$R = d_{5\mathrm{nn}}$	$R = d_{10\mathrm{nn}}$
Mega-masers	$4.6 \pm 2.8\%$	$0.4 \pm 1.6\%$	$0.3 \pm 1.6\%$	$0.13 \pm 1.5\%$
Masers	$6.1 \pm 2.6\%$	$0.9 \pm 2.4\%$	$0.6 \pm 2.1\%$	$0.31 \pm 1.9\%$
Control	$72 \pm 21\%$	$1.0 \pm 6.9\%$	$0.4 \pm 3.5\%$	$0.23 \pm 2.7\%$
	$R = 0.5$ Mpc	$R = 1$ Mpc	$R = 5$ Mpc	$R = 10$ Mpc
Mega-masers	$0.3 \pm 2.5\%$	$0.2 \pm 1.2\%$	$0.06 \pm 1.3\%$	$0.03 \pm 1.0\%$
Masers	$0.7 \pm 2.1\%$	$0.4 \pm 1.5\%$	$0.12 \pm 1.6\%$	$0.06 \pm 1.2\%$
Control	$0.7 \pm 2.2\%$	$0.3 \pm 1.6\%$	$0.07 \pm 1.4\%$	$0.04 \pm 1.3\%$

Table 3: Average number densities $\langle \rho \rangle$ (Mpc $^{-3}$) and associated fractional uncertainties calculated for fixed volumes determined by $R = d_{nn}$ and $R = 0.5$, 1, 5 and 10 Mpc, for objects in the flux-limited survey.

We show in Figure 6 the fractions of galaxies in bins of the number of neighbors detected in a given spherical volume. These calculations can be viewed as an alternative measure of the average densities corresponding to four different fixed-radius volumes around each maser or control galaxy. In a first approximation, the data show that for all of the volumes, the mega-maser and maser samples mimic the control sample properties. This suggests that maser detection is not strongly influenced by their environments, especially at large scales. The average density values listed in the second half of Table 3 support this conclusion, as they reveal little variation between maser and control average densities. However, the environments of the mega-maser galaxies appear less dense relative to the other galaxy populations, with the greatest difference being apparent in their very local neighborhoods ($R < 0.5 Mpc$).
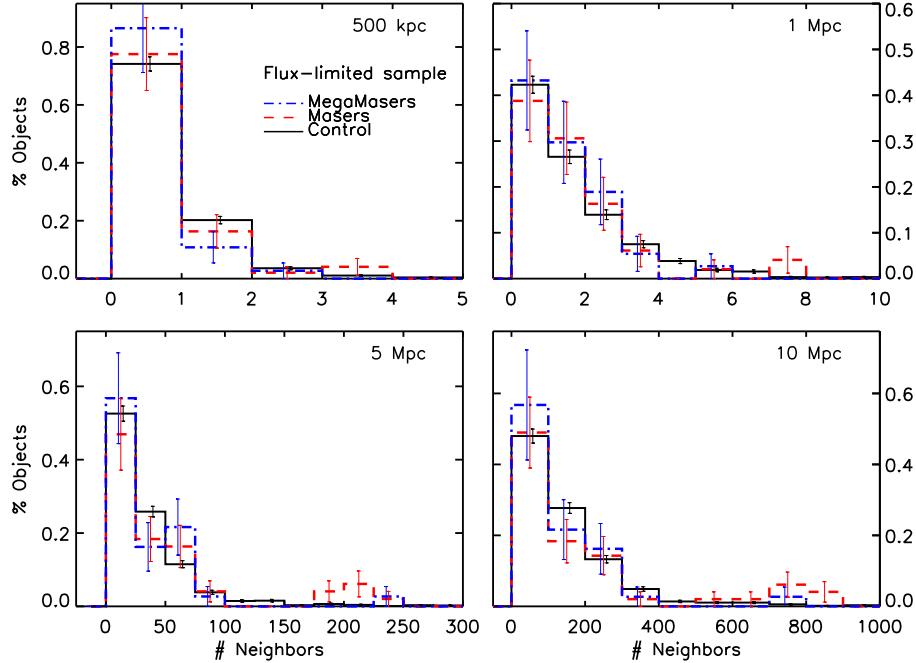
Fig. 6.— The fractions of mega-masers, masers and control objects as a function of total number of spec-z neighbors within a fixed volume ($R = 0.5, 1, 5,$ and 10 Mpc) for the flux-limited sample.

We also investigate the properties of the neighbors of mega-maser, maser and control galaxies in these four different volumes in Figure 7 and Figure 8, where we compare their $u - r$ color and M_r distributions respectively. The plots show that the neighbors of mega-maser and maser systems tend to be redder (larger $u - r$ colors) than those of the control galaxies, with the trend being more pronounced for the middle two volumes (especially for the 5 Mpc volume). While the error bars associated with each bin of the distributions overlap considerably in the first two volumes (500 kpc and 1 Mpc), and thus do not allow statistically significant conclusions, it remains apparent that there is an overall shift in the whole color distribution. Moreover, the closest neighbors of mega-masers span a much narrower range in colors, that is redder, in average than those of neighbors of the control systems. At the same time, the maser galaxies' neighbors tend to be slightly fainter while the mega-masers' neighbors
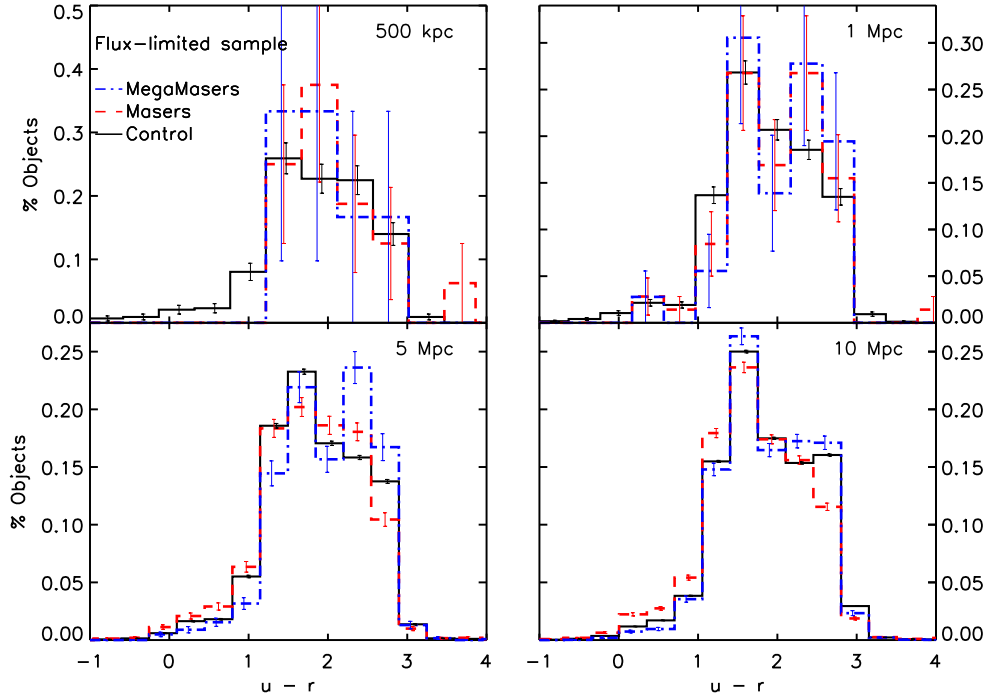
Fig. 7.— Distributions of $u - r$ colors of neighbors of mega-maser, maser and control, within the four fixed volumes.

are clearly on the bright side of the distributions. The differences tend however to be washed out for the largest volume possibly because, at this scale, the contributions of many different small scale environments are blended together in the final distribution.

3.3. Investigation of Close Companion Systems and their Properties

There is increasing evidence for the fact that galaxy-galaxy mergers and close interactions are a viable mechanism for channeling gas toward the central supermassive black holes (SMBHs) of galaxies which are triggered as active galactic nuclei (e.g., Darg et al. 2010). The angular-momentum loss that can
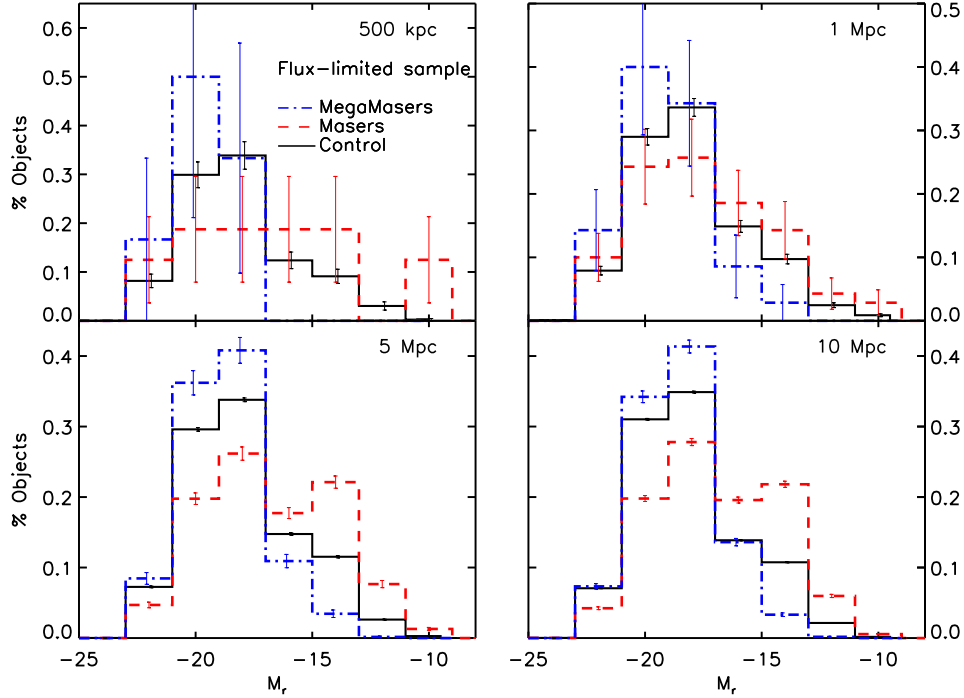
Fig. 8.— Distributions of absolute r-band magnitudes (M_r) for neighbors of mega-maser, maser and control, within the four fixed volumes.

take place in galactic interactions can allow for the infall of gas (Kewley et al. 2006) that fuels the central SMBH (Jogee 2008). AGN feedback can then control further infall and the cooling of gas, leading to reduced star formation (e.g., Khalatyan et al. 2008; Schawinski et al. 2009). It would thus be of interest to see to what degree the maser activity relates to these AGN-inducing environments, given that the majority of the mega-maser disks have been found in galaxies hosting AGN.

We investigate here the small scale environments of the maser and control galaxies with distances to their 1st nearest neighbor less than 500 kpc (a.k.a. companions) by looking at differences in the properties of these immediate neighbors. We consider their absolute r-band magnitudes M_r as well as their $u - r$ colors.
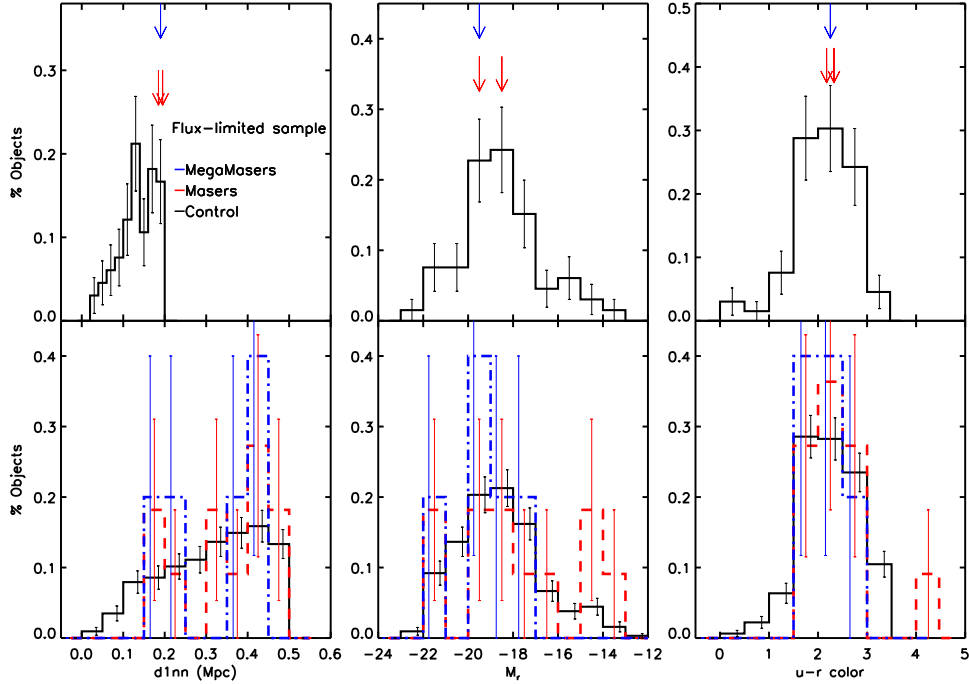
Fig. 9.— Distances to companions and companions' M_r and $u - r$ colors for the mega-masers, masers and control samples. Plots in the top row show the data for companions within < 200 kpc, while the plots in the lower row show measurements for companions within < 500 kpc. For the top row of plots, the bottom (red) arrows indicate locations of the two maser companions and the top (blue) arrows show the locations of the one mega-maser companion found within < 200 kpc (see Table 4).

Figure 9 and Table 4 present these data where the percentages given are of the associated sample size listed in Table 1. The most apparent trend is that the maser and mega-maser galaxies have significantly smaller numbers of companions than the control galaxies. Although the fraction of galaxies with companions within 0.2 Mpc are similar, the numbers of companions to maser and mega-maser galaxies are significantly lower, being almost nonexistent within 200 kpc; maser and mega-maser galaxies have no companions within 100 kpc. The comparison also shows that the closest companions (< 200 kpc) to the

maser galaxies are slightly more distant than the control companions, however the distributions become similar for the companions within 500 kpc. Interestingly, the M_r distributions for companions within 500 kpc show that the maser companions are fainter and redder than those of control galaxies, however, the mega-maser companions remain among the brightest (and probably more massive) and less red systems. These findings imply that the control galaxies live in slightly denser small scale environments, however, the connection between the mega-maser activity and close galaxy interactions remains ambiguous.

Table 4: Percent of each sample and the corresponding average distances to companions where d_{1nn} is within 0.1, 0.2 and 0.5 Mpc.

Sample	% < 0.1 Mpc	$\bar{d}$	% < 0.2 Mpc	$\bar{d}$	% < 0.5 Mpc	$\bar{d}$
Mega-masers	0	$\cdots$	3	0.19	14	0.33 ± 0.11
Masers	0	$\cdots$	4	0.18 ± 0.01	22	0.35 ± 0.11
Control	1	0.07 ± 0.02	5	0.13 ± 0.05	26	0.31 ± 0.12

4. Conclusions

We have analyzed here the environments of the galaxies hosting maser and mega-maser emission via a comparison of their nearest-neighbor statistics and properties with those of the neighbors of galaxies where maser emission was not detected, i.e., the control galaxies.

Based on comparisons of distributions of distances to first, third, fifth and tenth nearest neighbors, average densities based on volumes defined by nearest neighbor distances and on fixed volumes, and properties ($u - r$ colors and absolute r-band magnitudes M_r) of their neighbors, we find that, to a first approximation, both the small and the large scale environments of the control and the maser galaxies exhibit similar properties. Thus, the environment does not appear to play a crucial role in the detection rate of maser activity in galaxy centers. As such, we can conclude that environment need not be a priority when establishing search criteria for surveying for maser galaxies.

Although it seems that environment does not directly influence the mechanism responsible for maser emission, it is possible that the effects are not

negligible, because there are some notable differences in the properties of the environments of mega-maser, maser and control galaxies. Mainly: i) there is a higher fraction of mega-maser galaxies with less close companions (the mega-maser galaxies lack companions closer than 150 kpc) which suggests they prefer the lower density environments, and ii) the neighbors of masers appear redder and fainter than those of the control systems while the neighbors of mega-masers are brighter and more distant than those of masers and control galaxies. Together, these trends are complicated and do not provide a clear picture of which exact environmental feature might correlate best with the mega-maser phenomenon. It would be of benefit to work with larger samples of galaxies with spectroscopic redshifts in order to increase the number statistics and thus the confidence in these measurements.

REFERENCES

Bower, R. G., Benson, A. J., Malbon, R., Helly, J. C., Frenk, C. S., Baugh, C. M., Cole, S., & Lacey, C. G. 2006, MNRAS, 370, 645

Braatz, J. A., Reid, M. J., Humphreys, E. M. L., Henkel, C., Condon, J. J., & Lo, K. Y. 2010, ApJ, 718, 657

Carroll, S. M., Press, W. H., & Turner, E. L. 1992, ARA&A, 30, 499

Constantin, A., Hoyle, F., & Vogeley, M. S. 2008, ApJ, 673, 715

Constantin, A., & Vogeley, M. S. 2006, ApJ, 650, 727

Darg, D. W., Kaviraj, S., Lintott, C. J., Schawinski, K., Sarzi, M., et al. 2010, MNRAS, 401, 1043

Dressler, A. 1980, ApJ, 236, 351

Felli, M., Brand, J., Cesaroni, R., Codella, C., Comoretto, G., et al. 2007, A&A, 476, 373

Georgakakis, A., Gerke, B. F., Nandra, K., Laird, E. S., Coil, A. L., Cooper, M. C., & Newman, J. A. 2008, MNRAS, 391, 183

Greenhill, L. J., Henkel, C., Becker, R., Wilson, T. L., & Wouterloot, J. G. A. 1995, A&A, 304, 21

Herrnstein, J. R., Moran, J. M., Greenhill, L. J., Diamond, P. J., Inoue, M., et al. 1999, Nature, 400, 539

Jogee, S. 2008, The Fueling and Evolution of AGN: Internal and External Triggers, preprint (arXiv:0408383)

Kauffmann, G., White, S. D. M., Heckman, T. M., Ménard, B., Brinchmann, J., Charlot, S., Tremonti, C., & Brinkmann, J. 2004, MNRAS, 353, 713

Kewley, L. J., Geller, M. J., & Barton, E. J. 2006, AJ, 131, 2004

Khalatyan, A., Cattaneo, A., Schramm, M., Gottlöber, S., Steinmetz, M., & Wisotzki, L. 2008, MNRAS, 387, 13

Kondratko, P. T., Greenhill, L. J., & Moran, J. M. 2006, ApJ, 652, 136

Kuo, C. Y., Braatz, J. A., Condon, J. J., Impellizzeri, C. M. V., Lo, K. Y., et al. 2011, ApJ, 727, 20

Lo, K. Y. 2005, ARA&A, 43, 625

Miyoshi, S., Tanaka, N., Yoshimura, M., Yamashita, K., Furuzawa, A., Futamura, T., & Hudaverdi, M. 2005, Advances in Space Research, 36, 752

Reid, M. J., Braatz, J. A., Condon, J. J., Greenhill, L. J., Henkel, C., & Lo, K. Y. 2009, ApJ, 695, 287

Schawinski, K. 2009, in American Institute of Physics Conference Series, Vol. 1201, American Institute of Physics Conference Series, ed. S. Heinz & E. Wilcots, 17–20

Schawinski, K., Lintott, C. J., Thomas, D., Kaviraj, S., Viti, S., et al. 2009, ApJ, 690, 1672

Silverman, J. D., Kovač, K., Knobel, C., Lilly, S., Bolzonella, M., et al. 2009, ApJ, 695, 171

Zhu, G., Zaw, I., Blanton, M. R., & Greenhill, L. J. 2011, ApJ, 742, 73

_____

This preprint was prepared with the AAS LaTeX macros v5.2.